21st IMEKO TC4 International Symposium and
19th International Workshop on ADC Modelling and Testing
Understanding the World through Electrical and Electronic Measurement
Budapest, Hungary, September 7-9, 2016

A PSpice Model for Sensors Based on Stressimpedance Effect

Cristian Fosalau, Ionel Hogas, Cristian Zet, Daniel Petrisor

Technical University of Iasi, Faculty of Electrical Engineering
D.Mangeron 23, Iasi, Romania, cfosalau@tuiasi.ro

***Abstract* – In the paper, a new PSpice model aimed for simulating the stressimpedance effect in magnetic amorphous microwires is presented. The application of the model is made on a highly sensitive strain gage whose characteristic depends both on the applied strain and on the frequency of the current flowing through it. The characteristic to be modelled is a nonlinear surface representing a complex impedance, which has been implemented in PSpice using ABM functions, starting from the experimental characteristics of the sensor. The benefit of our modelling method is that it may be customized to a certain device exhibiting particular features, thus leading to a higher accuracy for a large range of operation. In our example, the surface was approximated by 2-variables polynomials, but, generalizing, any other type of functions may be employed for curve fitting. Another advantage of the method is that it can be extended to other devices nonlinearly working on spaces of more than 2 dimensions.**

***Keywords* – Spice model, strain gage, magnetic amorphous microwires, stressimpedance**

I. INTRODUCTION

It is well known that using simulating software in the electrical and electronic circuits design may be extremely useful for saving time and money and also for improving the circuit performances. The simulator packages utilize mathematical models for the devices involved in the design on the basis of which the program writes the circuit equation system, whose solutions represents the nodal voltages and the currents flowing through the circuit branches. The simulation performances are mainly assessed by the models' accuracy, i.e. the degree of approximation of the simulated quantity with respect to the real one. Usually, for building the device model one employs the mathematical equations that describe the device behaviour, if known. Else, one starts from the experimental characteristics from which empirical relationships are deduced. Using the device analytical equations is usually limited to certain input ranges on which the model fits the best to the real behaviour. Sometimes, even the nominal input range must be restricted in order to reach the best accuracy for the model. On the other hand, using real experimental characteristics for modelling depends on the measurement accuracy, implicitly on the employed instruments precision, on the suitability of the involved method, on the correct setting of the input-output correspondence, on the influence factors, etc. Actually, the model is deduced by device identification seen as a system. The benefit of the latter is that the model may be accurately accomplished even for devices exhibiting strong nonlinearities over a large span of inputs or working in difficult dynamic regimes. Once established the triad input-perturbation-output for the modelled system, its deploying into the simulating software may be easily carried out using the specific tool provided in the package.

Within the project PN-II-PT-PCCA-2011-3.2-0975, our research team has developed a new type of highly sensitive strain gage (HSSG) employed as sensitive elements for a landslide transducer working on three dimensions [1,2]. The operation of this gage relies on the stressimpedance effect (SI) occurring in the magnetic amorphous microwires (MAMW). This effect has been put in evidence for the first time in 1997 in amorphous ribbons and later in amorphous wires and consists in a large modification of a MAMW impedance under the action of a mechanical stress (strain) as the wire is fed by an ac current of several hundreds of kHz to several MHz [3-5]. This sensitivity to stress in amorphous magnetoelastic materials is assumed to be caused by changes of the internal magnetization state due to changes of magnetic permeability and magnetic anisotropy given by the helicoidal internal stresses frozen-in during the melting and rapid solidification in the in-rotating-water melt spinning fabrication technique [6,7].

We obtained for our strain gage a gage factor that exceeds 2000, i.e. 10 times bigger than that of a semiconductor one, over a range of ± 200 ppm. A drawback at a first glance of this device is the quite complex signal conditioning circuitry, as HSSG is

supplied with currents in the MHz range. Moreover, the gage impedance components nonlinearly depend both on axial stress and frequency, this leading to special cares when designing the circuit. The need of the model arose when we tried to design a signal conditioning circuit with frequency output and to obtain for it the optimal conditions of operation and maximum performances.

There are several reports on modelling and Spice simulation of another effect occurring in MAMW devices, the Giant Magnetoimpedance (GMI) effect, starting from the mathematical equations of the wire [9-11]. In [12] authors describe a model for GMI starting from experimental dependence of GMI on external applied magnetic field.

In this paper, we propose a model developed for an HSSG starting from the experimental dependence of MAMW active and reactive impedance components, *R* and *L* on axial tensile stresses and on current frequency. The application of this model was to design and optimize a signal conditioning circuit with frequency output. In the 2nd section of the paper we describe the construction, principle of operation and characteristics of the real strain gage on which basis we carried out the model. In the 3rd section we present the mathematical modelling derived from the characteristics fitting whilst in the 4th section we exemplify an implementation of the model in the Orcad's PSpice simulator. In the 5th section we assess the simulation goodness.

It is important to mention that our proposed method of modelling may be useful for building models for any other device nonlinearly working on surfaces or on spaces of more than two variables.

II. SENSOR CONSTRUCTION

The device construction is depicted in Fig. 1.

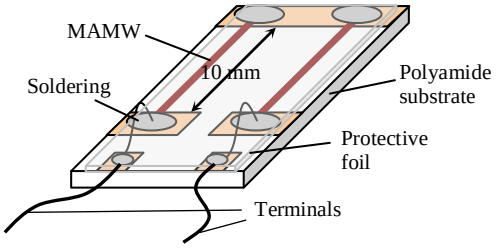

Fig. 1 Basic structure of an HSSG using MAMW

The sensitive element is represented by two Co-based MAMWs of 10 mm each, 120 μm diameter and composition of $(Co_{94}Fe_6)_{72.5}Si_{12.5}B_{15}$, electrically connected in series and bonded on a flexible plastic surface. The MAMWs are fabricated by "in-rotating quenching water method", being provided by the National Institute of Research and Development for Technical Physics Iasi. When a MAMW is fed by an ac current of frequencies over 100 kHz, the skin effect occurs, whose depth is given by [1]:

$$\delta = \sqrt{\frac{2\rho}{\omega\mu_{\Phi}(\sigma, H_{ext})}} \qquad (1)$$

where ρ is the material resistivity, ω is the current pulsation and $\mu_{\Phi_{\S}}$ is the circular permeability of the wire, which depends on the mechanical stress σ and on an external magnetic field, H_{ext}, axially applied to the MAMW. For a constant H_{ext},, according to the SI effect, the complex impedance is changing under the action of the axial stresses σ [1]:

$$Z = \frac{r}{2\sqrt{2\rho}} R_{dc}(1+j)\sqrt{\omega\mu(\sigma, H_{ext})} \qquad (2)$$

where r is the MAMW diameter and R_{dc} is the wire resistance in direct current. As it may be observed from (2), beside σ and H_{ext}, both active and reactive components of *Z* depend on the frequency *f* of the ac current that feeds the device. Indirectly, *Z* should also depend on the ac current intensity. It was experimentally proved, however, that this dependence is insignificant (under 0.2 %) for currents ranging between 0.5 to 5 mA.

With the aim of the gage modelling one considered the series equivalent schema of the device, as shown in Fig. 2.

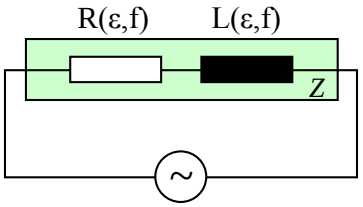

Fig. 2. The equivalent model of an HSSG

An experimental setup has been used for accurately controlling the HSSG axial tensile stress and for tracing the experimental dependences of the two components of *Z*, *R* and *L* vs. σ and *f* [1]. The measurements of *R* and *L* have been performed using an Agilent 4285A automated bridge. The axial stress range was -225 ppm to 225 ppm for a frequency span of 200 kHz to 2 MHz. The experimental characteristics underlying the model construction are presented in Figs. 3 and 4.

III. MATHEMATICAL MODELLING

In [9-11] authors propose the electrical model of the GMI effect in MAMWs starting from the mathematical description in (1) and (2). Thus, in [9] and [10] the model is based on the equivalent circuit of a Padé approximation derived from the impedance relied on Bessel functions.

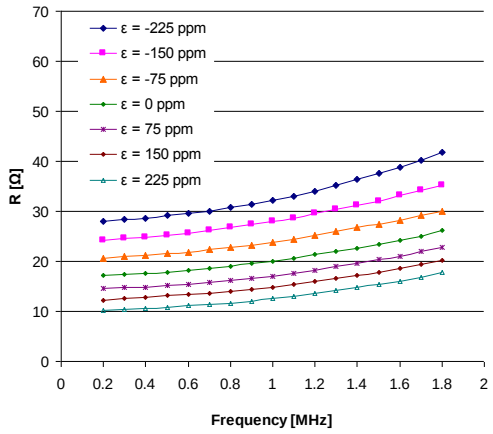

a)

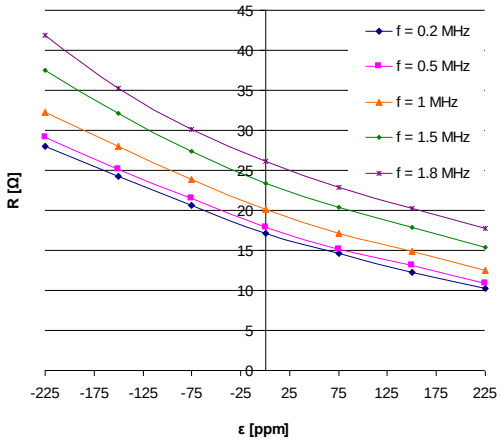

b)

Fig. 3. Dependence of the resistive component of the MAMW, R, on a) frequency and b) strain

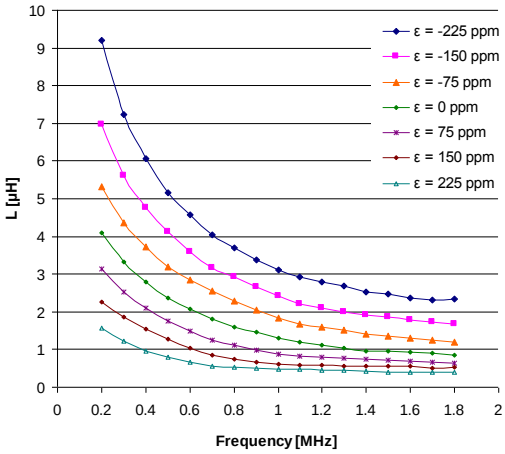

a)

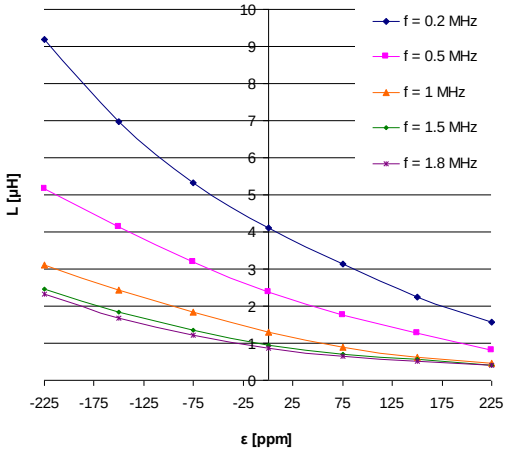

b)

Fig. 4. Dependence of the inductive component of the MAMW, L, on a) frequency and b) strain

In [11] the GMI sensors are mathematically studied using a new model based on polynomial functions involving zeros Bessel functions, its electrical implementation being realized using second-generation current conveyors, resistors, and inductors. Even if these models are designed to work over a large palette of frequencies and their implementation is very facile, they are strictly related to the accuracy of the general mathematical model depicted by (2), and they are not sensitive to changes of the MAMW structure and composition. In our approach, we developed a model for an SI sensor starting from the experimental characteristics of the material, being applicable for lots of individualized MAMWs and hence respecting much more accurately their real behaviour.

Moreover, the modelling method may be extended as a practical idea to other categories of sensors whose output nonlinearly depends on two or more parameters.

Coming back to the device described in section 2, the problem actually reduces to modelling two surfaces representing the dependences of the resistive and inductive components of Z on σ and f.

$$R = \zeta(\varepsilon, f); \quad L = \xi(\varepsilon, f) \tag{4}$$

In our experiment we decided to measure the stress by its effect over the MAMW, the strain ε, calculated as the relative elongation (for positive values) or compression (for negative values) with respect to the initial length of the wire:

$$\varepsilon = \frac{l - l_0}{l_0} 100 = \frac{\Delta l}{l_0} 100 \ [\%] \tag{5}$$

For an easy deployment of the model in Spice-like simulators, we chose the polynomial fitting method, being known that in PSpice this can be tailored with POLY(n) type Analog Behavioral Modelling (ABM) functions.

$$R(\varepsilon, f) = P_{R0} + P_{R1}\varepsilon + P_{R2} f + P_{R3}\varepsilon^2 + P_{R4}\varepsilon f + \\ + P_{R5} f^2 + P_{R6}\varepsilon^3 + P_{R7}\varepsilon^2 f + P_{R8}\varepsilon f^2 + P_{R9} f^3 + ... \quad (6)$$

$$L(\varepsilon, f) = P_{L0} + P_{L1}\varepsilon + P_{L2} f + P_{L3}\varepsilon^2 + P_{L4}\varepsilon f + \\ + P_{L5} f^2 + P_{L6}\varepsilon^3 + P_{L7}\varepsilon^2 f + P_{L8}\varepsilon f^2 + P_{L9} f^3 + ... \quad (7)$$

We have now to determine the values of P_{Ri} and P_{Lj} coefficients. On the other hand, (6) and (7) may be written as extended polynomial surfaces like:

$$R(\varepsilon, f) = \begin{bmatrix} 1 & f & ... & f^{M_R} \end{bmatrix} \times \begin{bmatrix} a_{00} & ..... & a_{N_R 0} \\ a_{01} & ..... & a_{N_R 1} \\ ..... & ..... & .... \\ a_{0M_R} & .... & a_{N_R M_R} \end{bmatrix} \times \begin{bmatrix} 1 & \varepsilon & ... & \varepsilon^{N_R} \end{bmatrix}^T \quad (8)$$

$$L(\varepsilon, f) = \begin{bmatrix} 1 & f & ... & f^{M_L} \end{bmatrix} \times \begin{bmatrix} b_{00} & ..... & b_{N_L 0} \\ b_{01} & ..... & b_{N_L 1} \\ ..... & ..... & . \\ b_{0M_L} & ... & b_{N_L M_L} \end{bmatrix} \times \begin{bmatrix} 1 & \varepsilon & ... & \varepsilon^{N_L} \end{bmatrix}^T \quad (9)$$

The calculation of a_{ij} and b_{ij} is described in the following. For every value f_k, the polynomial fitting was carried out by fixing $f = f_k$ and taking ε as variable, thus obtaining:

$$R_k(\varepsilon)\Big|_{f_k} = a_0(f_k) + a_1(f_k)\varepsilon + ... + a_{N_R}(f_k)\varepsilon^{N_R} \quad (10)$$

$$L_k(\varepsilon)\Big|_{f_k} = b_0(f_k) + b_1(f_k)\varepsilon + ... + b_{N_L}(f_k)\varepsilon^{N_L} \quad (11)$$

In order to obtain the polynomial coefficients $a_i(f_k)$ and $b_j(f_k)$ we also performed the polynomial fitting for every value of ε_l for which the characteristics were traced.

$$a_i(f) = a_{i0} + a_{i1} f + a_{i2} f^2 + ... + a_{iM_L} f^{M_L} \quad (12)$$

$$b_j(f) = b_{j0} + b_{j1} f + b_{j2} f^2 + ... + b_{jM_R} f^{M_R} \quad (13)$$

By replacing (12) and (13) in (10) and (11) and by properly arranging the terms according to (8) and (9), we can find the P_{Ri} and P_{Lj} coefficients.

IV. MODEL IMPLEMENTATION IN PSPICE

In order to implement the bidimensional surface in PSpice, we utilized the ABM functions type Polynomial Voltage Controlled POLY(2), which approximates the polynomial surfaces according to (6) and (7). Now, we need to identify the coefficients P_{Ri} and P_{Lj} among the coefficients a_{ij}. In this section we describe the working method starting from the example of the device described in section 2. Thus, equations (10) and (11) were best fit with 4-order polynomials, whereas (12) and (13) with 3-order ones. The goodness of fit is evaluated by calculating the parameter SSE (sum of square errors) that had minimum values for the above polynomial orders. The curve fitting procedure was performed using the Polynomial Fit function of LabVIEW. Below is given the correspondence for coefficient identification in R case. One proceeds similarly in L case.

$$\begin{bmatrix} a_{00} & a_{10} & a_{20} & a_{30} & a_{40} \\ a_{01} & a_{11} & a_{21} & a_{31} & a_{41} \\ a_{02} & a_{12} & a_{22} & a_{32} & a_{42} \\ a_{03} & a_{13} & a_{23} & a_{33} & a_{43} \end{bmatrix} \leftrightarrow \begin{bmatrix} P_{R0} & P_{R1} & P_{R3} & P_{R6} & P_{R10} \\ P_{R2} & P_{R4} & P_{R7} & P_{R11} & P_{R16} \\ P_{R5} & P_{R8} & P_{R12} & P_{R17} & P_{R23} \\ P_{R9} & P_{R13} & P_{R18} & P_{R24} & P_{R31} \end{bmatrix} \quad (14)$$

All coefficients up to P_{R31} that are not found in (14) are null. In Fig. 5 a), the block diagram of model implementation in PSpice is given. In the figure, FD is the frequency detector, VCL and VCR are voltage controlled inductance and resistance respectively, and EPOLY blocks are the ABM voltage controlled sources of 2 variables. Fig. 5 b) depicts the model symbol. In Fig. 5 c) the schematic of the frequency detector is presented.

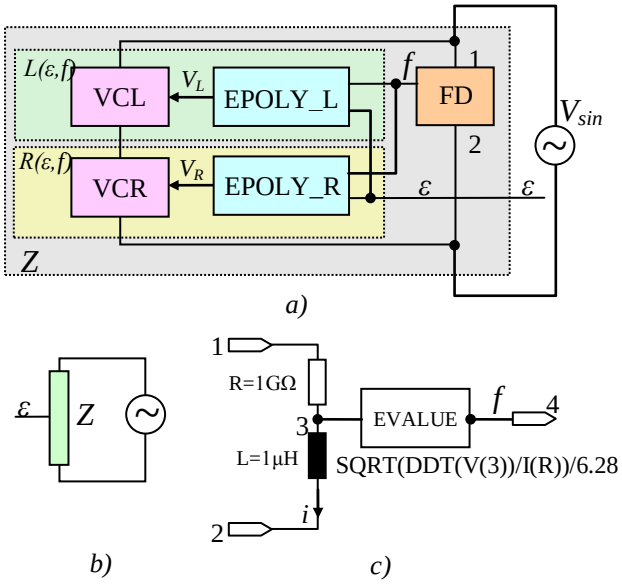

Fig. 5. a) Bloc diagram for PSpice model implementation, b) model symbol and c) schematic of the frequency detector.

The blocks VCL and VCR provide as output impedances controlled by the output voltages of EPOLY according to:

$$Z = V_{L(R)} Z_{ref} \tag{15}$$

where V_L and V_R are the controlling voltages and Z_{ref} is a reference of $Z_{ref} = R_{ref} = 1\Omega$ and $Z_{ref} = L_{ref} = 1H$.

Information about ac current frequency is obtained as a voltage whose value is equal with the frequency expressed in MHz. For this, one starts from the following relation valid for an ideal inductance:

$$\frac{du_L(t)}{dt} = (2\pi f)^2 Li(t) \Rightarrow f = \frac{1}{2\pi}\sqrt{\frac{\frac{du_L(t)}{dt}}{Li(t)}} \tag{16}$$

Eq. (16) is deployed in PSpice with the help of EVALUE function taken from ABM library, where, in Fig. 5 c), u_L is the voltage across the inductance L and i is the current flowing through the coil. The frequency detector should have a very high impedance in order to nor disturb the circuit operation, this being achieved by mounting the resistance R = 1 GΩ in series with L.

V. MODEL PERFORMANCE ASSESSMENT

In Fig. 6, the simulated characteristics are given against the experimental ones for the dependence of R and L on f, for ε = 75 ppm and ε = -150 ppm respectively. We chose for exemplification the above values because for them the worst behaviour of the model has been accomplished.

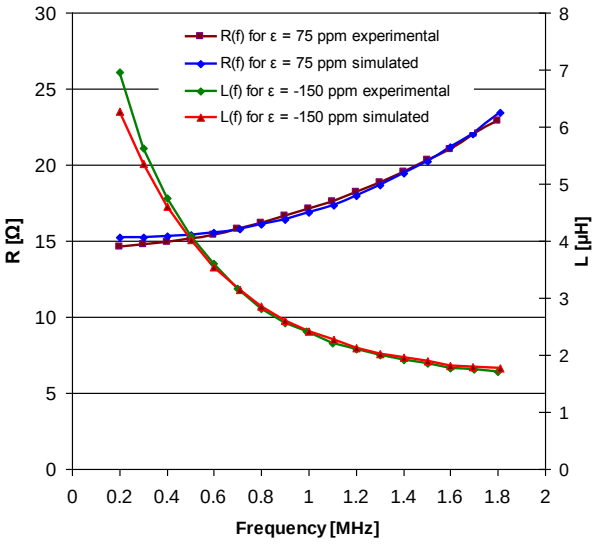

In order to appreciate the performances of the model, we carried out simulations of its behaviour in all points of the experimental characteristics considered in modelling stage. The simulations were performed in Cadence's Orcad PSpice v. 15.2. The model performance for a given set of simulation is assessed by calculating the root mean square relative error (*rmsre*) for every characteristic in a family:

$$rmsre = \sqrt{\frac{\sum_i \left(\frac{y_{s_i} - y_{\exp_i}}{y_{\exp_i}}\right)^2}{N}} \ [\%] \tag{17}$$

where y_{si} and y_{expi} are the values of R and L obtained by simulation and experimentally respectively, and N is the number of points in a characteristic (in our case, N = 17).

The results are shown in Table 1. In the table, the calculated values of *rmsre* are given for families of characteristics at which f is variable and ε is considered as a parameter. f took the same values the experimental characteristics were traced for, that is f = 0.2 to 1.8 MHz with steps of 100 kHz (17 values).

Table 1. Values of rmsre calculated for assessing the model performance

	ε [ppm]						
	-225	**-150**	**-75**	**0**	**75**	**150**	**225**
rmse$_R$ [%]	0.76	0.54	0.83	0.69	1.04	0.74	0.73
rmse$_L$ [%]	1.43	1.82	1.21	1.09	1.33	1.58	1.69

One may observe from the above table that the proposed model provides a quite good accuracy, the maximal error nod exceeding 2 %. The model behaves worse in the case of inductance simulation. The main sources of errors are the inaccuracies provided by the frequency detector, as it includes in its structure a derivative function and the polynomial curve fitting corectness.

VI. CONCLUSIONS

In the paper, a model suitable to be implemented in PSpice built on the basis of experimental characteristics traced for a sensor based on the stressimpedance effect is presented. The main advantage of the model is that it may be adapted to particular properties and working conditions of the device to be modelled, being useful when two ore more parameters influence its characteristics. Another benefit is that the model may be extended to devices whose characteristics are highly nonlinear surfaces of two or more variables.

VII. ACKNOWLEDGMENT

The results presented in this paper have been financially supported by the Romanian Ministry of Education and Research through the project PN-II-PT-PCCA-2011-3.2-0975, contract no. 63/2012.

REFERENCES

[1] Fosalau, C., Damian, C., and Zet, C., "A high performance strain gage based on the stress impedance effect in magnetic amorphous wires" Sensors and Actuators A: Physical, 191, pp. 105-110, 2013.

[2] Fosalau, C., Zet, C. and Petrisor, D., "Multiaxis inclinometer for in depth measurement of landslide movements", Sensor Review, vol. 35, no. 3, pp. 296-302, 2015.

[3] Deren Li, Zhichao Lu and Shaoxiong Zhou, "Giant stress-impedance effect in amorphous and thermally annealed $Fe_{73.5}Cu_1Nb_3Si_{13.5}B_9$ ribbons", Sensors and Actuators A: Physical, 109, Issues 1–2, pp. 68–71, 2003.

[4] Bayri, N. and Atalay, S., "Giant stress-impedance effect in $Fe_{71}Cr_7Si_9B_{13}$ amorphous wires", Journal of Alloys and Compounds 381 (S 1–2) pp. 245–249, 2004.

[5] Wan-Li Zhang, Bin Peng, Ding Su, Ru-Jun Tang and Hong-Chuan Jiang, "Stress impedance effects in flexible amorphous FeCoSiB magnetoelastic films", Journal of Magnetism and Magnetic Materials 320. pp. 1958–1960, 2008.

[6] Ogasawara, I. and Ueno, S., "Preparation and Properties of Amorphous Wires", IEEE Transactions on Magnetics, vol. 31, no.2, pp. 1219-1223, 1995.

[7] Hasegawa, R., "Magnetic wire fabrication and applications", Journal of Magnetism and Magnetic Materials 249, pp. 346–350, 2002.

[8] Morón, C., Carracedo, M.T., Zato, J.G. and García, A., "Stress and field dependence of the giant magnetoimpedance effect in Co-rich amorphous wires", Sensors and Actuators A: Physical, 106, Issues 1–3, pp. 217–220, 2003.

[9] De La Cruz Blas, C.A, Gomez-Polo, C., Carlosena, A. and Olivera, J., "A phenomenological spice model for magneto-impedance sensors", International Journal of Circuit Theory and Applications, vol. 40, Issue 3, pp. 275-286, 2012.

[10] De La Cruz Blas, C. A., Gomez-Polo, C., Carlosena, A. and Olivera, J., "A Spice model for magneto-impedance sensors", 52nd IEEE International Midwest Symposium on Circuits and Systems, MWSCAS '09, pp. 66-69, 2009.

[11] Vargas-Bernal, R., De la Cruz Blas, C.A. and Gómez-Polo, C., "A novel magneto-impedance sensor model based on the zeros of Bessel functions", International Journal of Circuit Theory and Applications, 43, Issue 12, pp. 2072-2080, 2015.

[12] Fosalau, C., Damian, C., and Zet, C., "PSpice Model for Simulating the Giant Magnetoimpedance Effect in Magnetic Amorphous Wires", Metrology and Measurement Systems, vol. XVI, no.1, 171-182, 2009.